DALTON
FULL PAPER

Electron-transfer kinetics and equilibria of copper(II/I) complexes with 1,4,7-trithiacyclononane. A square scheme mechanism involving ligand addition †

Ashoka Kandegedara,[a] Ksenia Krylova,[a] Timothy J. Nelson,[b] Ronald R. Schroeder,[a] L. A. Ochrymowycz[b] and D. B. Rorabacher *[a]

[a] *Department of Chemistry, Wayne State University, Detroit, MI 48202, USA. E-mail: dbr@chem.wayne.edu*
[b] *Department of Chemistry, University of Wisconsin at Eau Claire, Eau Claire, WI 54701, USA*

Received 16th August 2001, Accepted 19th October 2001
First published as an Advance Article on the web 24th January 2002

The electron-transfer kinetics of copper(II/I) complexes formed with the macrocyclic terdentate ligand 1,4,7-trithiacyclononane ([9]aneS$_3$ = TTCN = L) have been investigated under a variety of conditions. The relevant equilibrium constants, complex formation and dissociation rate constants, and redox potentials in both water and acetonitrile have also been determined. The predominant oxidized species in both solvents is $Cu^{II}L_2$, although the 1 : 1 complex, $Cu^{II}L(H_2O)_3$, can become dominant in water at high Cu(II) concentrations. The predominant reduced species is the 1 : 1 complex, $Cu^{I}L$ (*i.e.*, $Cu^{I}L(H_2O)$ or $Cu^{I}L(CH_3CN)$), as confirmed by electrospray mass spectrometry, pulsed square-wave voltammetry, cyclic voltammetry and the ligand dependence of the oxidation kinetics. Electron transfer occurs almost exclusively through the bis redox couple, $Cu^{II/I}L_2$, even for solutions containing predominantly $Cu^{II}L(H_2O)_3$. In the latter case, reduction involves a three-step sequence in which (i) $Cu^{II}L(H_2O)_3$ reacts with L to produce $Cu^{II}L_2$, (ii) electron transfer occurs and (iii) L dissociates again to yield $Cu^{I}L(H_2O)$. The sluggishness of direct electron transfer in the 1 : 1 complex is attributed to the unfavorable energetics of forming or dissociating strong copper–solvent bonds combined with the accompanying re-structuring of the surrounding solvent.

Introduction

The terdentate macrocycle 1,4,7-trithiacyclononane ([9]aneS$_3$ or TTCN) was first synthesized by Ochrymowycz and co-workers in 1977.[1] The three donor atoms in [9]aneS$_3$ are endodentate[2] with a geometric arrangement that facilitates the coordination of two ligand molecules to the opposite faces of an octahedral coordination sphere.[3] This unusual geometry has led to a large number of studies on the [9]aneS$_3$ complexes formed with a variety of metal ions in which the spectral properties and/or structures have been reported.[4] Takagi (Doine) and Swaddle have also studied the electron-transfer kinetics of the [9]aneS$_3$ complexes formed with Fe(III/II),[5] Co(III/II),[6] Pd(III/II),[7] Pt(III/II)[7] and Au(III/II).[7] In these latter systems it is presumed that the coordination geometry remains relatively constant during electron transfer.

[9]aneS$_3$ 

Wilson and co-workers[8] conducted the first study on the electron-transfer behavior of the Cu(II/I)–[9]aneS$_3$ system. Relying primarily on electrochemical studies, they concluded that electron-transfer involved a conformationally-controlled, dual-pathway square scheme mechanism of the type which we had previously proposed for Cu(II/I) complexes with larger macrocyclic tetrathiaether ligands (Fig. 1).[9–11] (The same mechanism has also recently been proposed by Takagi and co-workers for substituted bis(1,10-phenanthroline)copper(II/I) systems.[12–15])

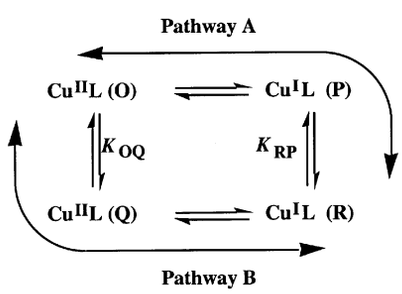

Fig. 1 Dual pathway square scheme mechanism proposed for electron transfer reactions involving Cu(II/I) complexes (ref. 9). The species designated as $Cu^{II}L(O)$ and $Cu^{I}L(R)$ represent the stable oxidized and reduced species, respectively, while $Cu^{II}L(Q)$ and $Cu^{I}L(P)$ represent metastable intermediates which are presumed to exhibit coordination geometries similar to their stable redox partners.

In their original study, Wilson *et al.* worked almost exclusively with solutions containing Cu : L concentration ratios of 1 : 2 based on the assumption that both the oxidized and reduced complex exist exclusively as the 1 : 2 species, $Cu^{II/I}L_2$, as observed in their crystal structures (Figs. 2A and 2B). In a subsequent paper,[16] they extended their studies to include pulse radiolysis in which they observed that a transient 1 : 1 $Cu^{II}L$ complex was initially formed upon oxidation; but they failed to recognize that the formation of this transient implies that the corresponding Cu(I) complex exists almost exclusively as the 1 : 1 complex in solution. No attempt was made to obtain specific electron-transfer rate constants.

Studies in our laboratory on the electron-transfer kinetic behavior of a wide variety of Cu(II/I) complexes with macrocyclic and acyclic polythiaether complexes[9–11,17–22] have shown that the use of small macrocyclic tetrathiaethers, which force

† Based on the presentation given at Dalton Discussion No. 4, 10–13th January 2002, Kloster Banz, Germany.

 DOI: 10.1039/b107449k

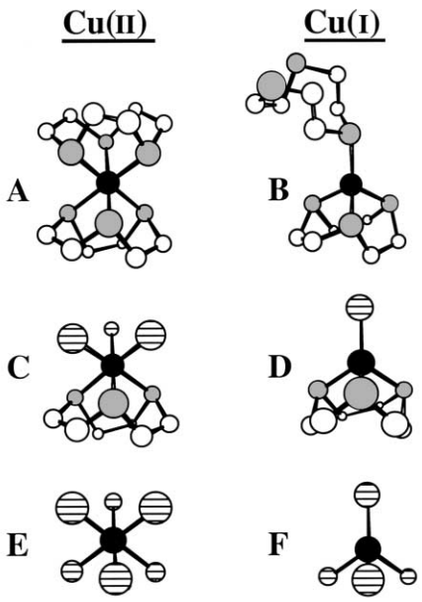

Fig. 2 Presumed structures for the various [9]aneS$_3$ (L) complexes formed with Cu(II) and Cu(I): (A) $Cu^{II}L_2$ and (B) $Cu^{I}L_2$, (C) $Cu^{II}L(H_2O)_3$, (D) $Cu^{I}L(H_2O)$, (E) $Cu^{II}(H_2O)_6$ and (F) $Cu^{I}(H_2O)_4$. Structures A and B are based on X-ray diffraction measurements of single crystals (ref. 8 and 34). For simplicity, Jahn–Teller distortion is omitted in the Cu(II) species.

the copper out of the donor atom plane, result in large electron self-exchange rate constants[23] equivalent to those observed for the most rapidly reacting blue copper proteins.[24] In these small macrocyclic complexes, a single Cu–S bond ruptures upon reduction of the copper with no required inversion of the other donor atoms. The structures in Fig. 2 suggest that reduction of $Cu^{II}([9]aneS_3)_2$ must be accompanied by the rupture of at least two Cu–S bonds, also without donor atom inversion. This fact, combined with the possibility of forming both 1 : 1 and 1 : 2 complexes with this ligand, suggested that a thorough study of the electron-transfer kinetics of $Cu^{II/I}([9]aneS_3)_n$ should be particularly enlightening.

The current investigation has included a wide variety of measurements including the determination of (i) the equilibrium constants associated with complex formation for Cu(II) and Cu(I), (ii) the corresponding complex formation and dissociation rate constants, (iii) the electrochemical behavior under a variety of conditions and (iv) the electron-transfer kinetics with several selected counter reagents. Both aqueous and acetonitrile solutions were included to permit the Cu : L ratio to be varied over a wide range. The resultant data show that the Cu(I) complex exists primarily as $Cu^{I}L$ (*i.e.*, $Cu^{I}([9]aneS_3)(H_2O)$ or $Cu^{I}([9]aneS_3)(CH_3CN)$) in solution (Fig. 2D) whereas Cu(II) is primarily present as the 1 : 2 complex, $Cu^{II}L_2$ (Fig. 2A). However, the corresponding 1 : 1 oxidized complex, $Cu^{II}L$ (*i.e.*, $Cu^{II}([9]aneS_3)(H_2O)_3$ represented by Fig. 2C), dominates in aqueous solutions containing very high copper concentrations. The overall electron-transfer behavior for the $Cu^{II/I}([9]aneS_3)_n$ system can be described in terms of a dual-pathway square scheme, but the resultant scheme is substantively different from that shown in Fig. 1 since the gain or loss of a ligand generally accompanies electron transfer. The effect of this latter feature upon the overall reaction kinetics is discussed.

Experimental

Reagents and solutions

The sample of 1,4,7-trithiacyclononane ([9]aneS$_3$) used in this work was synthesized by the modified procedure of Setzer *et al.*[3,25] which provides increased yields relative to our original synthetic approach.[1] The preparation of $Cu(ClO_4)_2$ and $NaClO_4$, the latter used for ionic strength control, has been previously described.[26] For studies in acetonitrile, the hydrated salts were recrystallized twice from acetonitrile before use and $Cu(CH_3CN)_4{\cdot}ClO_4$ was prepared by a modification of the method of Hathaway *et al.*[27] as described earlier.[28] (**CAUTION**! Perchlorate salts are potentially explosive and should be handled with care in small quantities. They should never be heated to dryness!) Most of the counter reagents used in this work were also prepared by literature methods as previously reported.[11] All aqueous solutions were prepared using conductivity-grade distilled-deionized water. Certified ACS grade acetonitrile (Fisher Scientific) was used as received. The addition of small amounts of water was shown to have no significant effect upon the observed kinetics.[29]

Although the [9]aneS$_3$ ligand exhibits limited solubility in water, aqueous solutions of up to 0.5 mM can be prepared. The concentrations of aqueous ligand stock solutions were determined spectrophotometrically by Hg(II) displacement mole-ratio plots in which aliquots of a standard Hg(II) solution were added to a series of solutions containing an excess of Cu^{II} over ligand:

$$Hg^{II} + Cu^{II}L_2 \longrightarrow Hg^{II}L_2 + Cu^{II} \qquad (1)$$

The absorbance of these solutions was measured at 445 nm (λ_{max} for $Cu^{II}L_2$) and the linearity of the resultant plot of absorbance *versus* Hg(II) concentration showed that the reaction was quantitative. The ligand concentration was taken as twice the concentration of Hg(II) required to achieve zero absorbance. The ligand concentrations determined in this manner proved to be virtually identical to those calculated from the weight of the ligand samples used. For solutions in acetonitrile, therefore, the concentration was based on the weight of ligand since the mercury displacement approach proved to be unsatisfactory in this solvent.

Instrumentation

Cyclic voltammograms of the $Cu^{II/I}L_n$ system and pulsed square-wave voltammetric data were obtained using a BAS 100 electrochemical work station (Bioanalytical Systems, Lafayette, IN, USA) operated at ambient temperature. All aqueous potentials were referenced to ferroin in 0.05 M NaCl (E^f = 1.117 V *vs.* SHE)[30] as an external standard while the potentials in acetonitrile were referenced to ferrocene (E^f = 0.400 V *vs.* SHE)[31] as either an internal or external standard. A three electrode electrochemical cell was used consisting of a 3 mm glassy carbon disc working electrode, a Pt wire auxiliary electrode and either a Ag/AgCl (3 M NaCl) or a saturated sodium calomel (SSCE) reference electrode (both from Bioanalytical Systems), the latter two electrodes having measured potentials of 0.226 and 0.262 V *vs.* SHE.[32] The glassy carbon electrode was polished with Micropolish Alumina 2 (Buehler) on a Microcloth Polishing Cloth (Buehler) for 60 s (30 s clockwise, 30 s counterclockwise) and then sonicated for 60 s in a small beaker filled with water or acetonitrile immersed in a Branson Ultrasonic Cleaner. This process was repeated with Micropolish Alumina 3. Formal potentials were taken as the half-wave potentials obtained from slow scan voltammograms (10–100 mV s^{-1}). More rapid scan rates were utilized when attempting to observe additional species under non-equilibrated conditions. The same instrumentation was utilized for the determination of the $Cu^{I}L_n$ stability constants by pulsed square-wave voltammetry (*vide infra*). Absorbance data for the stability constant determinations on the Cu(II) complexes were obtained using a Cary 17D double-beam recording spectrophotometer equipped with a thermostatted cell compartment.

Kinetic measurements

All kinetic measurements were made using one of two Durrum D-110 stopped-flow spectrophotometers interfaced to microcomputers with Metrabyte 12 bit A/D boards. The instrument used for measurements in acetonitrile was equipped with a modified flow system, designed and built by Tritech Scientific Ltd. of Winnipeg, Manitoba, Canada. This flow system contained all Teflon gaskets, thereby avoiding the leakage problems inherent when using acetonitrile in the original rubber gasket system. The temperature of all solutions was maintained at 25.0 ± 0.2 °C using a circulating water bath. The kinetic data were analyzed using software developed in house.

Results

As noted in the Introduction, both 1 : 1 and 1 : 2 complexes can be formed by [9]aneS$_3$ with with both Cu(II) and Cu(I). To facilitate discussion of this system, all forms of Cu(II) and Cu(I) in equilibrium with [9]aneS$_3$ in solution are represented in the stepladder scheme shown in Fig. 3. All Cu^{II} species are

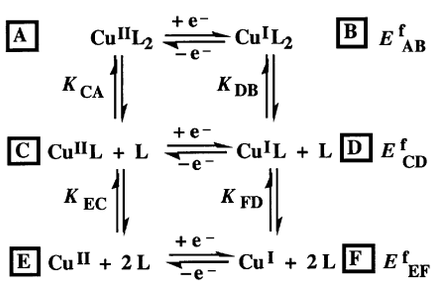

Fig. 3 Stepwise scheme defining the equilibria and potentials associated with the various oxidized and reduced species of copper ion in solutions containing [9]aneS$_3$ (L). The vertical reactions represent the association and dissociation of copper with the ligand while the horizontal processes represent electron transfer. Coordinated solvent molecules are omitted for simplicity.

presumed to be six-coordinate with solvent molecules occupying the remaining inner-sphere sites. Thus, in water Cu^{II} and $Cu^{II}L$ represent $Cu(H_2O)_6^{2+}$ [33] and $CuL(H_2O)_3)^{2+}$, respectively (Fig. 2C and 2E). Similarly, all Cu^{I} species are assumed to be four-coordinate so that Cu^{I} and $Cu^{I}L$ represent $Cu(H_2O)_4^{+}$ and $CuL(H_2O)^{+}$, respectively (Fig. 2D and 2F), in aqueous solution. To interpret the experimental electron-transfer kinetics, it was necessary to characterize the thermodynamic relationships between the various Cu(II) and Cu(I) species. Several novel approaches were employed for this purpose as described below.

Stability constant determinations for copper(II) complexes in water

The two stepwise equilibria for $Cu^{II}L_2$ formation are represented by the vertical reactions at the left side of Fig. 3:

$$Cu^{II} + L \underset{k_{CE}}{\overset{k_{EC}}{\rightleftharpoons}} Cu^{II}L \qquad K_1 = K_{EC} = \frac{[Cu^{II}L]}{[Cu^{II}][L]} \quad (2)$$

$$Cu^{II}L + L \underset{k_{AC}}{\overset{k_{CA}}{\rightleftharpoons}} Cu^{II}L_2 \qquad K_2 = K_{CA} = \frac{[Cu^{II}L_2]}{[Cu^{II}L][L]} \quad (3)$$

A spectrophotometric Job's plot for aqueous mixtures of Cu(II) and [9]aneS$_3$ showed a single maximum at 445 nm (λ_{max} for $Cu^{II}L_2$) [8] when the mole fraction of Cu^{II} was in the range of 0.25–0.33. No significant absorbance increase was noted at 374 nm (λ_{max} for $Cu^{II}L$). This is consistent with the expected formation of $Cu^{II}L_2$ as found in the crystal structure [34] (Fig. 2A) and implies that $Cu^{II}L_2$ is the dominant species in solution even in the presence of excess Cu(II), that is, $K_{CA} \gg K_{EC}$. Based on this observation, the overall equilibrium constant for the simultaneous coordination of two ligands to a single Cu^{II}, β_2, was determined directly in aqueous solutions containing Cu(II) and ligand:

$$\beta_2 = K_{EA} = \frac{[Cu^{II}L_2]}{[Cu^{II}][L]^2} = K_{EC}K_{CA} \quad (4)$$

using a modification of the spectrophotometric method of McConnell and Davidson: [35,36]

$$\frac{b\,C_{Cu(II)}}{A} = \frac{1}{\varepsilon_{Cu^{II}L_2}} + \frac{1}{\varepsilon_{Cu^{II}L_2}K_{EA}C_L^{\,2}} \quad (5)$$

In this expression, b represents the cell path length (in cm); A represents the measured absorbance at 445 nm; $\varepsilon_{Cu^{II}L_2}$ represents the molar absorptivity of the $Cu^{II}L_2$ complex at this wavelength; and $C_{Cu(II)}$ and C_L are the mass balance relationships for Cu(II) and ligand, respectively:

$$C_{Cu(II)} = [Cu^{II}] + [Cu^{II}L] + [Cu^{II}L_2] \quad (6)$$

$$C_L = [L] + [Cu^{II}L] + 2\,[Cu^{II}L_2] \quad (7)$$

where it was assumed that the $[Cu^{II}L]$ term is not significant under these conditions. A plot of $bC_{Cu(II)}/A$ *vs.* C_L^2 at 25 °C, μ = 0.10 M, showed excellent linearity with $\beta_2 = K_{EA} = 2.57 \times 10^{10}$ M^{-2} as the intercept-to-slope ratio and $\varepsilon_{CuL_2} = 9.4 \times 10^3$ M^{-1} cm^{-1} as the reciprocal intercept.

From pulse radiolysis experiments on the Cu(I) complex in aqueous solution, Wilson and co-workers observed a transient species with $\lambda_{max} \approx 370$ nm.[16] This species reportedly decayed with a half life of 7.65 ms (for $C_{Cu(I)}$ = 0.1 mM and C_L = 0.2 mM) [16] to produce $Cu^{II}L_2$ as confirmed by the growth of the peak at 445 nm. The transient species was identified as the 1 : 1 complex, $Cu^{II}L$. In the current work we have shown that the conproportionation reaction:

$$Cu^{II} + Cu^{II}L_2 \rightleftharpoons 2\,Cu^{II}L \quad K_{eq}^{\,II} \quad (8)$$

can be forced far to the right for solutions in which $C_{Cu(II)} >$ 10 mM $\gg C_L$. Under such conditions, eqns. (6) and (7) reduce to $C_{Cu(II)} \approx [Cu^{II}]$ and $C_L = [Cu^{II}L] + 2[Cu^{II}L_2]$, respectively, to yield the expression:

$$K_{eq}^{\,II} = \frac{K_{EC}}{K_{CA}} = \frac{[Cu^{II}L]^2}{[Cu^{II}][Cu^{II}L_2]} \approx \frac{\{C_L - 2[Cu^{II}L_2]\}^2}{C_{Cu}[Cu^{II}L_2]} \quad (9)$$

The absorbance of $Cu^{II}L_2$ was monitored at 445 nm as a function of $C_{Cu(II)}$ (at very high concentration) for solutions containing constant C_L to generate a mean value of $K_{eq}^{\,II} = 7.5 \times 10^{-3}$ at 25 °C, μ = 0.10 M. Measurement of the same solutions at 374 nm revealed that $\varepsilon_{Cu^{II}L} = 2.9 \times 10^3$ M^{-1} cm^{-1} at the latter wavelength. The stepwise equilibrium constants for reactions 2 and 3 were then calculated as follows:

$$K_{EC} = (K_{EA}\,K_{eq}^{\,II})^{1/2} = 1.38 \times 10^4\ M^{-1} \quad (10)$$

$$K_{CA} = K_{EA}/K_{eq}^{\,II} = 1.86 \times 10^6\ M^{-1} \quad (11)$$

These results are consistent with our conclusion that $K_{CA} \gg K_{EC}$.

Formation and dissociation rate constants for copper(II) complexes

As an independent check on the K_{EC} value, we determined the formation rate constant, k_{EC}, for the $Cu^{II}L$ complex (reaction 2) by mixing Cu^{II} and L in a stopped-flow spectrophotometer. The absorbance data obtained at 374 nm with Cu(II) in large excess were shown to conform to the pseudo-first-order rate expression:[37]

$$\frac{d[Cu^{II}L]}{dt} = k_{obs}[L] \quad (12)$$

where

$$k_{obs} = k_{EC}[Cu^{II}] + k_{CE} \quad (13)$$

Although the kinetic behavior appeared to be consistently pseudo-first-order over the majority of the reaction,[38] only the initial portion of the data was utilized to minimize errors which might be induced by a loss of $Cu^{II}L$ due to the formation of $Cu^{II}L_2$ (reaction 3). The resolved rate constants obtained from a plot of k_{obs} *vs.* $[Cu^{II}]$ yielded $k_{EC} = (1.2 \pm 0.2) \times 10^5$ M^{-1} s^{-1} as the slope and $k_{CE} = 30 \pm 8$ s^{-1} as the intercept.[39] As an additional check for data consistency, the value of the $Cu^{II}L$ dissociation rate constant, k_{CE}, was also determined independently at 374 nm by mixing Hg(II)—as a scavenger ion[39]—with solutions containing ligand plus very high concentrations of Cu(II) (to generate primarily $Cu^{II}L$):

$$Cu^{II}L \xrightarrow{k_{CE}} Cu^{II} + L \qquad \text{rate determining} \quad (14a)$$

$$L + {}^1/_2\,Hg^{II} \rightarrow {}^1/_2\,Hg^{II}L_2 \qquad \text{fast} \quad (14b)$$

As noted earlier, the reaction of Hg^{II} with the copper complex is quantitative so that the foregoing reaction proceeded to completion. In previous determinations of the dissociation rate constants for copper(II) complexes of this type using mercury(II) displacement,[39,40] we have noted that the reaction kinetics often exhibit some dependence on the Hg^{II} concentration, indicating that a portion of the reaction proceeds through an intermediate in which Hg^{II} interacts with the ligand prior to complete $Cu^{II}L$ dissociation:

$$Cu^{II}L + Hg^{II} \xrightarrow{k_{Hg}} Cu^{II}LHg^{II} \qquad \text{rate determining} \quad (15a)$$

$$Cu^{II}LHg^{II} \rightarrow Cu^{II} + Hg^{II}L \qquad \text{fast} \quad (15b)$$

For such systems, the overall kinetic behavior conforms to the expression:

$$-\frac{d[Cu^{II}L]}{dt} = \{k_{CE} + k_{Hg}[Hg^{II}]\}[Cu^{II}L] = k_{app}[Cu^{II}L] \quad (16)$$

A plot of k_{app} *vs.* $[Hg^{II}]$ yielded an intercept of $k_{CE} = 16.6 \pm 0.9$ s^{-1} which is considered to be a much more reliable value than that obtained from the study of the formation kinetics (*i.e.*, $k_{CE} = 30 \pm 8$ s^{-1}). The ratio of $k_{EC}/k_{CE} = 7.2 \times 10^3$ M^{-1} is one-half the magnitude of the K_{EC} value determined from eqn. (10). This disagreement is presumed to represent experimental error since four independent measurements were involved.

It was not possible to obtain direct kinetic measurements on the formation of the $Cu^{II}L_2$ complex from $Cu^{II}L$ (reaction 3). However, by mixing $Cu^{II}L_2$ with excess Hg^{II} and monitoring the disappearance of $Cu^{II}L_2$ at 445 nm, the kinetics for the dissociation of $Cu^{II}L_2$ (k_{AC} in reaction 3) could be obtained in a manner analogous to reaction 14 where Hg(II) rapidly scavenged the free ligand as shown in reaction 14b. The kinetic behavior was analogous to eqn. (16). Extrapolation of the apparent pseudo-first-order rate constant, k_{app}, to zero Hg^{II} concentration yielded $k_{AC} = 1.4 \pm 0.2$ s^{-1} as the intercept. From our values of k_{AC} and K_{CA}, we estimate that $k_{CA_0} \approx 2.6 \times 10^6$ M^{-1} s^{-1}, about 25 times larger than k_{EC}. This is in good agreement with a value of $k_{CA} \geq 1.3 \times 10^6$ M^{-1} s^{-1} as calculated from the observed half-lifetime reported by Wilson and co-workers for the conversion of $Cu^{II}L$ to $Cu^{II}L_2$ following pulse radiolysis.[16] (Their reported value of $k_{CA} = 8.4 \times 10^5$ M^{-1} s^{-1} appears to be inconsistent with their observed half-life.)

The values of K_{CA} and K_{EC} could not be determined by the same methods in acetonitrile, principally due to the fact that these constants are much larger in the nonaqueous solvent.[28] Instead, the relevant acetonitrile values were estimated from other data as noted below.

Nature of the copper(I) complexes in acetonitrile

The crystal structure of the $Cu^{I}([9]aneS_3)_2$ complex ion[8] showed that one ligand was coordinated to copper through all three sulfur donor atoms while the second ligand was attached by a single Cu–S coordinate bond (Fig. 2B). This observation caused Wilson and co-workers to conclude that the Cu(I) complex exists primarily as $Cu^{I}L_2$ in solution with the two ligands unequally coordinated.[8,16] However, studies in our laboratory have shown that any complex involving a singly bonded thioether ligand is of very low stability.[41] Thus, the second ligand can be easily displaced by a solvent molecule to generate $Cu^{I}L(solv)$. To confirm this hypothesis, we carried out a series of electrospray mass spectrometry experiments in acetonitrile to permit the use of higher ligand concentrations. Even in a solution containing a 200-fold excess of ligand ($C_{Cu(I)} = 0.03$ mM, $C_L = 6.6$ mM), the intensity of the mass peak corresponding to CuL_2^+ (M = 283.76) is only about 1% of that for the peak corresponding to $CuL(CH_3CN)^+$ (M = 422.75).[42] The limited solubility of $[9]aneS_3$ in water did not allow the generation of such concentrated ligand solutions. However, evidence to support the fact that $Cu^{I}L(H_2O)^+$ is the dominant Cu(I) species in aqueous solution includes (i) the observed ligand dependence of the oxidation kinetics in water and (ii) the computer simulations of the cyclic voltammetric behavior (*vide infra*).

The Osteryoung pulsed square-wave voltammetric method[43] was applied to acetonitrile solutions containing Cu(I) and varying amounts of ligand in an attempt to evaluate the equilibrium constant between the $Cu^{I}L$ and $Cu^{I}L_2$ species:

$$Cu^{I}L + L \rightleftharpoons Cu^{I}L_2 \qquad K_{DB} = \frac{[Cu^{I}L_2]}{[Cu^{I}L]\,[L]} \quad (17)$$

For this purpose, the current for the peak corresponding to the oxidation of $Cu^{I}L_2$ can be related to the $Cu^{I}L_2$ concentration by the relationship:[28]

$$i_p = \left\{\frac{nFA\sqrt{D_0}[Cu^{I}L_2]}{\sqrt{\pi\tau}}\right\}\Delta\psi_p = y[Cu^{I}L_2] \quad (18)$$

where i_p is the peak current, n is the number of electrons transferred in the reaction, F is the Faraday constant, A is the surface area of the working electrode, D_0 is the diffusion coefficient for $Cu^{I}L_2$, τ is the pulse period, and $\Delta\Psi_p$ is the current function at the peak potential. Under conditions where the total ligand concentration is in excess over Cu(I) (so that the concentration of free Cu(I) is insignificant), eqns. (17) and (18) can be combined with the mass balance equations for Cu(I) and ligand (analogous to eqns. (6) and (7)) to yield:

$$\frac{C_{Cu(I)}}{i_p} = \frac{1}{y} + \frac{1}{yK_{DB}(C_L - C_{Cu(I)} - [Cu^{I}L])} \quad (19)$$

Iterative corrections for $[Cu^{I}L]$ in eqn. (19) resulted in a plot of $C_{Cu(I)}/i_p$ *vs.* $(C_L - C_{Cu(I)} - [Cu^{I}L])$ for which the

intercept-to-slope ratio yielded $K_{DB} \approx 650\ M^{-1}$ in acetonitrile at 23 °C, $\mu = 0.10$ M.

Cyclic voltammetric measurements

Extensive cyclic voltammetric (CV) measurements were made on both $Cu^{II}L_n$ and $Cu^{I}L_n$ solutions in which the Cu(II) concentration was varied over a 2500-fold range, 0.20–500 mM (as contrasted to the six-fold variation reported by Wilson and co-workers);[8] only a sampling of the CV data will be discussed here. Under equimolar conditions ($C_{Cu(II)} = 0.20$ mM $= C_L$), the voltammograms appear to be reversible with a single cathodic peak at 362 mV (E_{pc}) and a single anodic peak at 420 mV (E_{pa}) (*vs.* Ag/AgCl–NaCl). At a Cu(II) concentration of 0.80 mM, the main anodic peak appears at more positive potentials (465 mV) and, as the scan rate is increased, continues to move more positively while a second anodic peak emerges at lower potential and finally becomes dominant at about 430 mV (Fig. 4). The

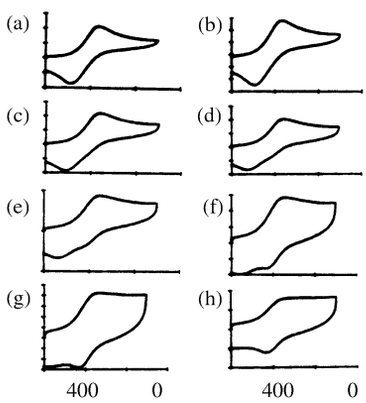

Fig. 4 Effect of scan rate on cyclic voltammograms of $Cu^{II}([9]aneS_3)_n$ in water (potentials are in mV *vs.* Ag/AgCl (3 M NaCl)): $C_{Cu(II)} = 0.80$ mM, $C_L = 0.20$ mM, $\mu = 0.10$ M ($HClO_4$). Scan rates are as follows (V s^{-1}): (a) 0.050, (b) 0.100, (c) 0.250, (d) 0.500, (e) 1.00, (f) 2.50, (g) 5.00, (h) 10.0.

lone cathodic peak remains invariant. When the total Cu(II) concentration is increased 100-fold to 80 mM, the main cathodic peak appears at a more positive potential (430 mV) and the lone anodic peak is at 505 mV, but a second smaller cathodic peak becomes evident at 245 mV (Fig. 5). As the scan rate is

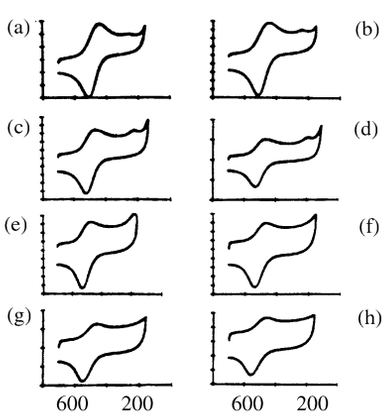

Fig. 5 Effect of scan rate on cyclic voltammograms of $Cu^{II}([9]aneS_3)_n$ in water (potentials are in mV *vs.* Ag/AgCl (3 M NaCl)): $C_{Cu(II)} = 80$ mM, $C_L = 0.20$ mM, $\mu = 0.24$ M ($Cu(ClO_4)_2$). Scan rates are as follows (V s^{-1}): (a) 0.050, (b) 0.100, (c) 0.250, (d) 0.500, (e) 1.00, (f) 2.50, (g) 5.00, (h) 10.0.

increased, the latter cathodic peak moves to more negative potentials and eventually merges with the plating peak for elemental copper. At the highest Cu(II) concentration tested, 0.50 M ($\mu = 1.5$ M), the slow scan voltammograms (50 mV s^{-1}) are reversible with the cathodic and anodic peaks at 410 and 475 mV, respectively, corresponding to the 430 and 505 mV peaks described for 80 mM Cu(II)—the negative shift being attributable to the large increase in ionic strength. As the scan rate is increased in this last case, the peaks spread but no other features are noted.

For reduced aqueous solutions initially containing equimolar Cu(I) and [9]aneS$_3$ (0.20 mM each), slow scan CV's show a single anodic peak at 485 mV and a single cathodic peak at 385 mV. At higher scan rates, the anodic peak moves to about 505 mV while the cathodic peak remains virtually invariant. When 20 mM Cu(II) is added to a solution containing both Cu(I) and [9]aneS$_3$ at 0.20 mM, a reversible voltammogram is observed at slow scan rates with cathodic and anodic peaks at 430 and 505 mV, respectively, while a second cathodic peak is also apparent at about 220 mV (Fig. 6). The latter

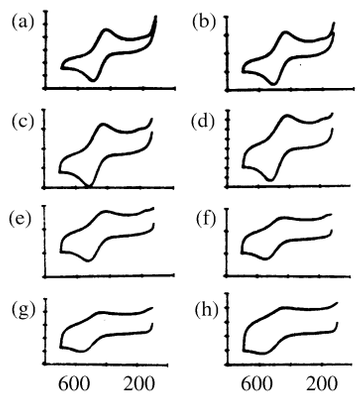

Fig. 6 Effect of scan rate on cyclic voltammograms of $Cu^{I}([9]aneS_3)_n$ in water (potentials are in mV *vs.* Ag/AgCl (3 M NaCl)): $C_{Cu(II)} = 20$ mM, $C_{Cu(I)} = C_L = 0.20$ mM, $\mu = 0.16$ M ($Cu(ClO_4)_2$). Scan rates are as follows (V s^{-1}): (a) 0.050, (b) 0.100, (c) 0.250, (d) 0.500, (e) 1.00, (f) 2.50, (g) 5.00, (h) 10.0.

peak becomes more prominent as the Cu(II) concentration is increased to 0.50 M.

The foregoing voltammetric behavior, together with the calculated equilibrium constants described above, can be used to assign the peaks as follows. The initially observed cathodic peak at 362 mV represents the reduction of equilibrated $Cu^{II}L_2$/$Cu^{II}L$. The shift of the cathodic peak to 430 mV at very high Cu(II) concentration represents the greater dominance of $Cu^{II}L$ to this equilibrated peak under these conditions. The small cathodic peak appearing at 220–245 mV is more difficult to assign but is presumed to arise from the direct reduction of aquated Cu^{2+} followed by coordination with a free ligand molecule:

$$Cu^{II} + L + e^- \longrightarrow Cu^{I}L \qquad (20)$$

In the case of the anodic peaks, the peak initially observed at 420 mV for low Cu(II) concentrations represents the equilibrated peak for $Cu^{I}L_2$ and $Cu^{I}L$. Although $Cu^{I}L$ is dominant in solution, the greater ease of oxidizing $Cu^{I}L_2$ makes the peak appear at a potential which essentially represents the 1 : 2 species. At higher Cu(II) concentrations, the peaks appearing at 505 mV and 430 mV are assigned as the oxidation peaks for $Cu^{I}L$ and $Cu^{I}L_2$, respectively.

Computer simulation of the cyclic voltammograms was carried out using DigiSim software (Bioanalytical Systems, West Lafayette, IN). For the simulations, a value of $\alpha = 0.5$ was assigned and the diffusion coefficient was assumed to be 10^{-5} cm^2 s^{-1}. Introduction of the equilibrium constants, rate constants and potentials determined experimentally (Table 1) yielded all of the features observed in the voltammetric curves—including the small cathodic peak in the vicinity of

Table 1 Physical properties for the $Cu^{II/I}([9]aneS_3)_n$ system in water and in acetonitrile at 25 °C, $\mu = 0.10$ M (ClO_4^-)

Parameter	Water	Acetonitrile
λ_{max} ($Cu^{II}L_2$)/nm	445	*same*[d]
$\varepsilon_{Cu^{II}L_2}$/M^{-1} cm^{-1}	9.3×10^3	*same*
λ_{max} ($Cu^{II}L$)/nm	374	*same*
$\varepsilon_{Cu^{II}L}$/M^{-1} cm^{-1}	2.9×10^3	*same*
k_{EC}/M^{-1} s^{-1}	$(1.2 \pm 0.2) \times 10^5$	
k_{CE}/s^{-1}	16.6 ± 0.9,[a] 30 ± 8[b]	
k_{CA}/M^{-1} s^{-1}	*2.6×10^6*[d]	
k_{AC}/s^{-1}	1.4 ± 0.2[a]	
K_{EC}/M^{-1}	1.38×10^4	
K_{CA}/M^{-1}	1.86×10^6	$\approx 10^8$
K_{FD}/M^{-1}	*9×10^{13}*[d]	
K_{DB}/M^{-1}	*$\approx 4 \times 10^3$*[d]	6.5×10^2
E_{EF}^f/V[c]	0.13	0.66
E_{CD}^f/V[c]	0.72	0.54
E_{AB}^f/V[c]	*0.65*[d]	*0.29*[d]
E_{AD}^f/V[c]	0.41	0.12

[a] Based on the use of Hg^{II} as a scavenger for the ligand. [b] Intercept from formation kinetic studies. [c] Aqueous potentials are *vs.* SHE; acetonitrile potentials are *vs.* ferrocene. [d] Values in italics were not determined directly but were calculated from other parameters within this table.

220–245 mV—when K_{DB} was assigned a value of about 4×10^4 M^{-1} and $E_{AB}^f \approx 0.65$ V (see Fig. 3). The latter two values are included in Table 1 and have been applied to the subsequent analysis of the electron-transfer kinetics.

Formal potentials

Formal potential values for the $Cu^{II/I}L_n$ system were determined in both water and acetonitrile as the half wave potentials from slow scan cyclic voltammetry (10–100 mV s^{-1}) containing appropriate concentrations of copper and ligand. Cyclic voltammograms of equimolar mixtures of $[Cu^I(CH_3CN)_4](ClO_4)$ and ligand at very high concentrations ($\approx 10^{-2}$ M) in acetonitrile showed two distinct cathodic peaks representing the reduction of $Cu^{II}L$ and $Cu^{II}L_2$, respectively. The former peak and the lone anodic peak were used to estimate a value of $E_{CD}^f = 0.54$ V (*vs.* ferrocene). In more dilute solutions, the cathodic peak representing the reduction of $Cu^{II}L_2$ to Cu^IL was dominant:

$$Cu^{II}L_2 + e^- \rightleftharpoons Cu^IL + L \qquad E_{AD^f} \qquad (21)$$

As expected, the half wave potential was found to vary with the concentration of excess ligand:

$$E_{1/2} = E_{AD}^f + \frac{2.303\,RT}{F}\log[L] \qquad (22)$$

Extrapolation to [L] = 1.0 M yielded a value of $E_{AD}^f = 0.12$ V (*vs.* ferrocene) in acetonitrile with a slope of 0.0508, in reasonable agreement with the theoretical slope of 0.0592. Combination of this value with the value of $K_{DB} = 650$ M^{-1} yields $E_{AB}^f = 0.29$ V (*vs.* ferrocene) in acetonitrile. The voltammograms for acetonitrile solutions which contained only solvated copper yielded $E_{EF}^f = 0.66$ V (*vs.* ferrocene). From these potentials and $K_{DB} = 650$ M^{-1}, the value of K_{CA} is estimated to be about 10^8 M^{-1} in acetonitrile.

In aqueous media, the cyclic voltammograms for solutions containing very high concentrations of Cu^{II} (up to 0.5 M) and dilute ligand gave a value of $E_{CD}^f = 0.72$ V (*vs.* SHE). At lower Cu^{II} concentrations ($<10^{-4}$ M), the potential for the A ⇌ D redox couple (reaction 21) showed the expected dependence on the ligand concentration. Extrapolation to [L] = 1.0 M, indicated that the value of E_{AD}^f was in the range of 0.36–0.41 V (*vs.* SHE), but the data were relatively imprecise. As noted above, digital simulation of the cyclic voltammograms over a wide range of conditions were consistent with $K_{DB} \approx 4 \times 10^3$ M^{-1} and $E_{AB}^f \approx 0.65$ V. The aqueous concentration potential for E_{EF}^f has previously been calculated to be 0.13 V at 25 °C, $\mu = 0.10$ M (*vs.* SHE).[44] From these potentials and the values previously determined for E_{CD}^f and K_{CA}, the aqueous K_{FD} value was calculated to be 9×10^{13} M^{-1}. This latter value is in general agreement with a large number of similar Cu^IL stability constants in aqueous solution.[32]

All of the foregoing formation/dissociation rate constants, equilibrium constants and redox potentials are summarized in Table 1 for both water and acetonitrile.

Electron-transfer kinetics

The main goal of this investigation was to determine the mechanism for electron transfer and the corresponding self-exchange rate constants, k_{11}, characteristic of the $Cu^{II/I}([9]aneS_3)_n$ system under varying conditions. Based on the equilibrium studies, it is apparent that, except in aqueous media containing very high concentrations of Cu(II), the predominant species in solution are $Cu^{II}L_2$ (A) and Cu^IL (D). The oxidized and reduced copper complexes were reacted with a variety of reductants (A_{Red}) and oxidants (A_{Ox}) to examine the kinetic behavior and determine the cross reaction rate constants, k_{12} and k_{21}:

$$Cu^{II}L_2 + A_{Red} \underset{k_{21}}{\overset{k_{12}}{\rightleftharpoons}} Cu^IL + L + A_{Ox} \qquad (23)$$

In these studies, the Cu : L ratio was varied over a relatively wide range. Since the loss or gain of a ligand may either precede or succeed the electron transfer step, the overall kinetic behavior can be formulated in terms of the dual-pathway square scheme shown in Fig. 7. This scheme is reminiscent of

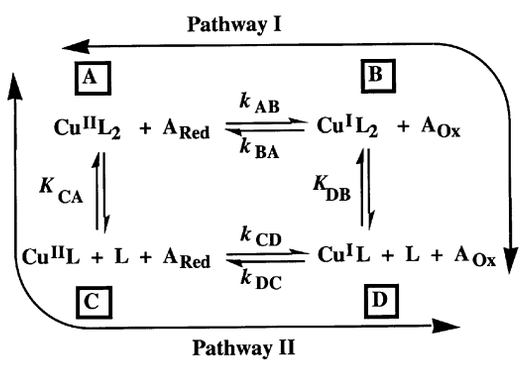

Fig. 7 Dual-pathway square scheme mechanism for electron transfer involving the $Cu^{II/I}([9]aneS_3)_n$ system. The vertical reactions involve ligand gain or loss while the horizontal reactions represent electron transfer.

the square scheme mechanism which we have previously proposed for Cu(II/I) systems involving macrocyclic polythiaethers (Fig. 1).[9–11,17,21,45] However, in Fig. 7 the intermediate steps involve the addition or loss of a ligand rather than a specific conformational change.

Electron-transfer kinetic studies involving excess copper were conducted exclusively in aqueous solution (since the solvated copper ion itself is electroactive in acetonitrile). Kinetic studies involving excess ligand were conducted in both water and acetonitrile with the highest ligand concentration studies restricted to the latter solvent. All parameters for the counter reagents used in this work are summarized in Table 2 for both water and acetonitrile. For all cross reaction studies, the k_{12} and k_{21} values were resolved for kinetic runs involving four or five different reactant concentrations (each concentration condition involving approximately eight replicate runs). The mean k_{12} or k_{21} value for each reaction studied was then used to calculate the apparent k_{11} values using the Marcus cross relation[46] as described elsewhere.[9]

$$*Cu^{II}L_2 + Cu^IL \underset{}{\overset{k_{11}}{\rightleftharpoons}} *Cu^IL + Cu^{II}L_2 \qquad (24)$$

Table 2 Physical properties of counter reagents used in this work for electron-transfer kinetic studies with $Cu^{III/II}([9]aneS_3)_n$ in both aqueous and acetonitrile solutions at 25 °C, $\mu = 0.10$ M

Counter reagent[a]	E^f in H_2O[b]/ V (*vs.* SHE)	E^f in CH_3CN[c]/ V (*vs.* Fc)	k_{22} in H_2O/ $M^{-1}\ s^{-1}$	k_{22} in CH_3CN/ $M^{-1}\ s^{-1}$	$10^8\ r$[c]/ cm	λ_{max}[d]/ nm	$10^{-4}\ \varepsilon$/ $M^{-1}\ cm^{-1}$
Reductants							
$Ru^{II}(NH_3)_4bpy$	0.526	0.127	2.2×10^6[e]	5.5×10^5[c]	4.4	522 ± 2	0.331[e]
$Ru^{II}(NH_3)_4phen$	0.536		2.2×10^6[f]		4.4	471 ± 2	0.757[g]
$Ru^{II}(NH_3)_5isn$	0.405	−0.012	1.1×10^5[e]	4.7×10^5[c]	3.8	478 ± 2	1.19[e]
Oxidants							
$Ru^{III}(NH_3)_2(bpy)_2$	0.889[h]		8.4×10^7[e]		5.6	292 ± 2	5.88[i]
$Ni^{III}([9]aneN_3)_2$	0.972	0.555	6.0×10^3[b]	2.1×10^3[b]	4.5	312 ± 2[j]	1.11[b]
$Fe^{III}(4,7\text{-}Me_2phen)_3$	0.921	0.538	3.8×10^8[k]	3.0×10^7[c]	6.6	512 ± 2	1.40[l]

[a] Ligand abbreviations: bpy = 2,2′-bipyridine; phen = 1,10-phenanthroline; isn = isonicotinamide; [9]aneN$_3$ = 1,4,7-triazacyclononane; 4,7-Me$_2$phen = 4,7-dimethyl-1,10-phenanthroline. [b] This work. [c] Refs. 20 and 29. [d] Absorbance peaks listed refer to the reduced complexes except as noted. [e] Ref. 47. [f] k_{22} assumed to be identical to that of $Ru^{III/II}(NH_3)_4bpy$. [g] Ref. 48. [h] Ref. 49. [i] Ref. 50. [j] Absorbance peak is for the oxidized complex. [k] Ref. 51. [l] Ref. 52.

Table 3 Mean cross reaction rate constants and calculated self-exchange rate constants for $Cu^{III/II}([9]aneS_3)_n$ reacting with selected reductants and oxidants in aqueous solution at 25 °C

Counter reagent	Reagent concentration/μM	C_{Cu}/μM	C_L/μM	$10^{-6}\ k_{12}$ (or k_{21})/$M^{-1}\ s^{-1}$	log (k_{11}/$M^{-1}\ s^{-1}$)[a]
Reductants					
$Ru^{II}(NH_3)_4bpy$	19–151	2.8	33.4	1.9 ± 0.4[b]	4.98
$Ru^{II}(NH_3)_4phen$	4.29–28.4	4.9	93	9.7 ± 0.4[c]	6.21
$Ru^{II}(NH_3)_5isn$	1.72–17.2	3.01	45.0	11 ± 2[c]	5.75
Oxidants					
$Ni^{III}([9]aneN_3)_2$	251–403	4.8	93	0.35 ± 0.04[b]	1.54
$Ru^{III}(NH_3)_2(bpy)_2$	1.49–2.98	3.01	45.0	23 ± 2[c]	2.44
$Fe^{III}(4,7\text{-}Me_2phen)_3$	3.97–13.2	4.9	95	114 ± 30[c]	2.87

[a] Calculated using $E_{measd} \approx 0.6$ V for $Cu^{II}L_2/Cu^{II}L$. [b] Kinetic data were resolved as pseudo-first-order. [c] Kinetic data were resolved as second-order.

Table 4 Mean cross reaction rate constants and calculated self-exchange rate constants for $Cu^{III/II}([9]aneS_3)_n$ reacting with selected reductants and oxidants in acetonitrile at 25 °C, $\mu = 0.10$ M ($NaClO_4$)

Counter reagent	Reagent concn/μM	C_{Cu}/μM	C_L/μM	$10^{-6}\ k_{12}$ (or k_{21})/$M^{-1}\ s^{-1}$	log (k_{11}/$M^{-1}\ s^{-1}$)[a]
Reductants					
$Ru^{II}(NH_3)_4bpy$	18.8–43.2	2.31	34.0	0.93 ± 0.07[b]	3.61
	14.1–100	23.1	455	0.9[b,d]	3.61
	14.1–90.3	23.1	525	1.2[b,d]	3.87
$Ru^{II}(NH_3)_5isn$	3.78–15.9	2.31	34.0	14 ± 2[b]	4.05
Oxidants					
$Ni^{III}([9]aneN_3)_2$	111–412	2.31	34.0	0.00289 ± 0.00001[c]	−1.4
	202–939	5.15	2550	0.271 ± 0.005	2.93
$Fe^{III}(4,7\text{-}Me_2phen)_3$	0.355–4.31	2.31	34.0	0.14 ± 0.03[b]	−1.2
	2.32–6.51	5.15	52.5	0.7[b,d]	−0.7
	1.21–9.8	5.15	525	5[b,d]	1.3

[a] Calculated using $E_{measd} \approx 0.27$ V for $Cu^{II}L_2/Cu^{II}L$. [b] Kinetic data were resolved as second-order. [c] Kinetic data were resolved as pseudo-first-order. [d] Data were scattered; value reported is the median.

Aqueous kinetic studies with excess ligand

In aqueous solution, the reaction kinetics were studied under conditions in which the ligand was present in 10- to 20-fold excess over the total copper. Three reductants and three oxidants were used as counter reagents. The calculated k_{12} or k_{21} values are tabulated in Table 3. Calculation of the electron self-exchange rate constant, k_{11}, with the Marcus cross relation was based on the measured Cu(II/I) potential for the specific conditions utilized. For studies involving $Cu^{II}L_2$ reduction ($k_{11(Red)}$), the value of k_{11} calculated from the reaction with $Ru^{II}(NH_3)_4bpy$ differs from the values obtained from the other two reductions by about an order of magnitude. Our final evaluation of the "corrected" electron self-exchange rate constants suggests that the rate constant obtained with $Ru^{II}(NH_3)_4bpy$ may be too small (see Discussion.) The self-exchange rate constant values obtained for $Cu^{I}L$ oxidation, $k_{11(Ox)}$, in the presence of excess ligand, are clearly within experimental error, particularly since the k_{21} value for the fastest of these reactions exceeded $10^8\ M^{-1}\ s^{-1}$.

An independent kinetic study was conducted in acetonitrile to permit the use of higher ligand concentrations. In these experiments, the ligand was always maintained in at least a 10-fold excess over the concentration of copper with two reductants and two oxidants being used as counter reagents (Table 4). For one reductant, $Ru^{II}(NH_3)_4bpy$, the total ligand concentration was increased by 10-fold with no discernible effect upon the resolved k_{12} value. For the oxidation reactions with $Fe^{III}(4,7\text{-}Me_2phen)_3$ and $Ni^{III}([9]aneN_3)_2$, the ligand concentration was increased by one and two orders of magnitude, respectively. As is evident from the data in Table 4, the latter studies indicate that the apparent cross reaction rate constant for the oxidation of $Cu^{I}L$ increases proportionately with the increase in ligand concentration.

Under conditions in which the Cu(II) ion was present in huge excess (0.25 M) in aqueous solution, the pseudo-first-order rate

constants for the reduction of $Cu^{II}L$ with $Ru^{II}(NH_3)_4bpy$ were determined for solutions in which the total ligand concentration was varied by 10-fold while maintaining at least a 10-fold excess of ligand over the counter reagent. Under these conditions, the observed first-order rate constant increased at a faster pace than did the ligand concentration. The implications of this observation are discussed in the next section.

Discussion

The equilibrium constant data in Table 1 reveal that the dominant species in solution are $Cu^{II}L_2$ and $Cu^{I}L$ except when the metal ion is present in very high concentrations. As illustrated in Fig. 7, the reduction of $Cu^{II}L_2$ (A) to $Cu^{I}L$ (D) must involve ligand dissociation either following the electron-transfer step (Pathway I) or preceding it (Pathway II); and the inverse two-step process will take place during oxidation. If the addition and loss of the second ligand is sufficiently rapid to maintain equilibrium between the mono and bis complexes, the effect of ligand concentration upon the electron-transfer kinetics can be examined to determine the favored reaction pathway. Thus, if Pathway I is dominant, the rate of $Cu^{I}L$ oxidation (D ⟶ B ⟶ A) should increase with excess ligand concentration whereas the reduction rate for $Cu^{II}L_2$ (A ⟶ B ⟶ D) should be ligand independent—since ligand loss would occur after the electron-transfer step. Conversely, if Pathway II is dominant, the rate of $Cu^{II}L_2$ reduction (A ⟶ C ⟶ D) should show an inverse dependence upon ligand concentration whereas the oxidation of $Cu^{I}L$ (D ⟶ C ⟶ A) should be independent of ligand effects—since ligand addition would then follow electron transfer.

Reaction pathways

The rate dependence on ligand concentration was examined in acetonitrile in the presence of a large excess of ligand to insure that the ligand concentration would remain relatively constant throughout the reaction. As shown by the data in Table 4, the cross reaction rate constant data for the reduction of $Cu^{II}L_2$ by $Ru^{II}(NH_3)_4bpy$ showed no evidence of a significant ligand concentration dependence. By contrast, the apparent cross reaction rate constant, k_{21}, for the oxidation of $Cu^{I}L$ with $Fe^{III}(4,7\text{-}Me_2phen)_3$ showed a significant increase with increasing ligand concentration. The effect of increasing ligand concentration is even more pronounced in the case of the oxidation reaction with $Ni^{III}([9]aneN_3)_2$ where a 100-fold increase in the concentration of $[9]aneS_3$ caused a 100-fold increase in the observed k_{21} value. Therefore, we conclude that, under normal circumstances, Pathway I is the preferred reaction path.

For the oxidation reaction with $Fe^{III}(4,7\text{-}Me_2phen)_3$, it was further shown that the reaction was first-order with respect to the Fe^{III} complex. This demonstrates that the addition of a second ligand to $Cu^{I}L$ (*i.e.*, step D ⟶ B) did not become the rate-limiting step. Thus, we conclude that, in this study at least, $Cu^{I}L_2$ (B) was in rapid equilibrium with $Cu^{I}L$ (D).

Although Pathway I appears to be the favored pathway in the presence of excess ligand, it was unclear whether the reaction might switch to Pathway II in the presence of a huge excess of Cu(II), where $Cu^{II}L$ (C) becomes the predominant oxidized species in solution. At a Cu(II) concentration of 0.25 M, the $Cu^{II}L_2$ species still represents 4.5% of the complexed Cu(II) in solution if the total ligand concentration is 10^{-4} M. However, this can be reduced to 0.5% of complexed Cu(II) when the total ligand concentration is 10^{-5} M. As noted earlier, the hydrated Cu(II/I) couple is virtually redox inactive since the outer-sphere electron self-exchange rate constant is reported to be 5×10^{-7} M^{-1} s^{-1},[53] too small to contribute to the observed cross reaction kinetics with counter reagents, provided that inner-sphere pathways are prevented. Thus, when large concentrations of excess Cu(II) are present, the dominant electron-transfer cross reaction can be represented as:

$$Cu^{II}L + A_{Red} \underset{k_{21}}{\overset{k_{12}}{\rightleftharpoons}} Cu^{I}L + A_{Ox} \qquad (25)$$

To determine the dominant pathway, the kinetics of $Cu^{II}L$ reacting with $Ru^{II}(NH_3)_4bpy$ were studied in solutions containing 0.25 M Cu(II) under conditions in which the total ligand concentration was varied from about 10- to 100-fold excess over the Ru(II) reagent and the reaction was monitored by following the loss of Ru^{II}. If the reaction were to proceed by Pathway II (C ⟶ D), the rate expression would be:

$$-\frac{d[Ru^{II}]}{dt} = k_{CD}[Ru^{II}][Cu^{II}L] \qquad (26)$$

Since $[Cu^{II}L] \approx C_L$ and $C_L \gg [A_{Red}]$, the resulting pseudo-first-order expression would be:

$$-\frac{d[A_{Red}]}{dt} = k_{obs}[A_{Red}] \qquad (27)$$

where

$$k_{obs} = k_{CD}\, C_L \qquad (28)$$

By contrast, if Pathway I were the dominant reaction path, the expected rate equation would be:

$$-\frac{d[Ru^{II}]}{dt} = k_{AB}[Ru^{II}][Cu^{II}L_2] \qquad (29)$$

Substitution of eqn. (9) for $[Cu^{II}L_2]$, where $[Cu^{II}L] \approx C_L$ and $[Cu^{II}] \approx C_{Cu}$, yields:

$$-\frac{d[Ru^{II}]}{dt} = k_{AB}[Ru^{II}]\frac{C_L^{\,2}}{k_{eq}^{II} C_{Cu(II)}} = k_{obs}[Ru^{II}] \qquad (30)$$

where

$$k_{obs} = \frac{k_{AB} C_L^{\,2}}{K_{eq^{II}} C_{Cu(II)}} \qquad (31)$$

In Fig. 8, the resolved pseudo-first-order rate constants for $Ru^{II}(NH_3)_4bpy$ reacting with $Cu^{II}L$ are plotted against both C_L (eqn. (28)) and C_L^2 (eqn. (31)). It is clear that the latter relationship is linear, indicating that the reaction is proceeding by

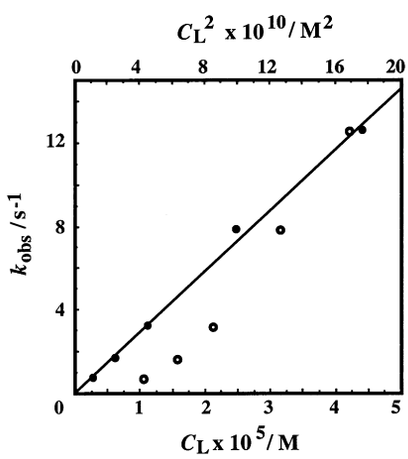

Fig. 8 Plot of observed pseudo-first-order rate constant for the oxidation of $Cu^{II}([9]aneS_3)$ with $Ru^{II}(NH_3)_4bpy$ in water: $C_{Cu(II)} = 0.25$ M, $C_{Ru(II)} = 1.51$ μM, $C_L = 10.5$–42.0 μM, 25 °C, $\mu = 0.80$ M ($HClO_4$). The open circles are plotted against the total ligand concentration, C_L (bottom scale) while the solid circles are plotted against C_L^2 (top scale).

Table 5 "Corrected" electron self-exchange solvents for the $Cu^{II}L_2/Cu^{I}L_2$ redox couple after compensation for the equilibrium with the $Cu^{I}L$ species

Counter reagent	log (k_{11}/M^{-1} s^{-1})	
	Water[a]	Acetonitrile[b]
Reductants		
$Ru^{II}(NH_3)_4$bpy	4.19 (5.95)[c]	3.35, 3.32, 3.57
$Ru^{II}(NH_3)_4$phen	5.64	
$Ru^{II}(NH_3)_5$isn	5.05	3.74
Oxidants		
$Ni^{III}([9]aneN_3)_2$	3.18	2.35, 3.21
$Ru^{III}(NH_3)_2(bpy)_2$	4.84	
$Fe^{III}(4,7\text{-}Me_2phen)_3$	4.60	2.50, 3.64, 3.16

[a] Calculated using E_{AB}^{f} = 0.65 V (H_2O) for $Cu^{II}L_2/Cu^{I}L_2$. [b] Calculated using E_{AB}^{f} = 0.29 V (CH_3CN) for $Cu^{II}L_2/Cu^{I}L_2$. [c] Value calculated from the reduction kinetics of $Cu^{II}L$ in the presence of 0.25 M Cu(II) after compensation for the equilibrium with $Cu^{II}L_2$.

Pathway I (*i.e.*, C ⟶ A ⟶ B ⟶ D). Based on the slope of the linear plot in Fig. 8 (7.3×10^9) and the known values of K_{eq}^{II} (7.5×10^{-3}) and $C_{Cu(II)}$ (0.25 M), the value of k_{AB} is estimated to be 1.4×10^7 M^{-1} s^{-1}. This latter value presumes that $Cu^{II}L$ and $Cu^{II}L_2$ are in equilibrium throughout the reaction. However, in light of the very small concentration of free ligand in solution, we estimate that the rate of C ⟶ A is in approximately the same range as the rate of A ⟶ B under the prevailing reaction conditions. (This possibility is further indicated by the fact that, when Ru^{II} was maintained in excess over the total ligand concentration in the presence of 0.25 M Cu(II), biphasic kinetics were observed.) Nonetheless, even if the reaction were controlled by the C ⟶ A step, the reaction would still depend upon C_L^2 since both [$Cu^{II}L$] and [L] increase in direct proportion to the total ligand concentration. Thus, the linearity of the plot of k_{obs} *vs.* C_L^2 (Fig. 8) is diagnostic for Pathway I.

A reasonable estimate of the self-exchange rate constant for the AB redox couple (*i.e.*, for $Cu^{II}L_2/Cu^{I}L_2$) designated as $k_{11(AB)}$ (reductions) or $k_{11(BA)}$ (oxidations), can be obtained from the apparent self-exchange rate constants listed in Table 3 by the following relationships:

$$k_{11(AB)} = k_{11(Red)}' \quad (32)$$

$$k_{11(BA)} = K_{DB}\,[L]\,k_{11(Ox)} \quad (33)$$

where $k_{11(Red)}'$ is the self-exchange rate constant calculated from the Marcus relationship using the potential value for E_{AB}^{f} rather than the measured potential for A ⇌ D under the prevailing conditions (the latter values having been applied for the calculated k_{11} values listed in Table 4). The resulting values for $k_{11(AB)}$ are listed in Table 5 for both the acetonitrile and aqueous studies. Similarly, the values for $k_{11(BA)}$ can be estimated from the oxidation kinetic data using eqn. (33) in which the product K_{DB}[L] represents an equilibrium preceding the electron-transfer step. In both solvents, the calculated $k_{11(AB)}$ values are within experimental error of the $k_{11(BA)}$ values. In aqueous solution, these "corrected" k_{11} values are approximately 10^5 M^{-1} s^{-1}. Thus, the electron self-exchange rate constant for the bis-[9]-aneS_3 complex in aqueous solution is among the largest values observed for Cu(II/I) systems.[23]

When $C_{Cu(II)}$ = 0.25 M, both the calculated k_{12} and k_{21} values are reduced by about 100–200-fold (prior to compensation for the mono to bis complex) relative to the values obtained when ligand was present in excess. For the reduction reactions, this is commensurate with the fact that the $Cu^{II}L_2$ concentration is also reduced by about 200-fold. Since this evidence implies that Pathway I dominates even under these adverse conditions, the direct self-exchange rate constant for the $Cu^{II}L/Cu^{I}L$ (C/D) redox couple must be *much* smaller than the self-exchange rate constant for the $Cu^{II}L_2/Cu^{I}L_2$ (A/B) redox couple. The sluggishness of the electron-transfer process for the $Cu^{II}L/Cu^{I}L$ (C/D) redox couple may reflect some of the same influences which account for the very small k_{11} value associated with the fully aquated Cu(II/I) couple since both systems require the loss of two coordinated water molecules. In a recent study on a Cu(II/I)-tripodal ligand system,[54] in which a strongly coordinated water molecule is lost during reduction, a similarly small k_{11} value was obtained.

The generation of $Cu^{II}L$ directly from $Cu^{I}L$ under the extreme conditions of pulse radiolysis, as observed by Wilson and co-workers,[16] indicates that Pathway II is viable. This type of behavior is analogous to the change in reaction pathway which we have observed for Cu(II/I)–tetrathiaether complexes where ligand conformational changes are involved during the electron-transfer process.[11–13,45] In those reactions, we have been able to access intermediate driving conditions in which the conformational change itself becomes rate-limiting so that the reaction is independent of the concentration of counter reagent, the condition known as "gated" electron transfer. In our current studies on the reduction of $Cu^{II}L$ in the presence of high Cu(II) concentrations, it appears that we are on the verge of a somewhat analogous condition in which the reaction of $Cu^{II}L$ with free ligand to produce $Cu^{II}L_2$ prior to electron transfer could become the rate-limiting process. Since the latter situation is dependent upon the concentration of a second reagent, namely, free ligand, it is biologically analogous to an enzymatic reaction in which the limited availability of a co-factor controls the rate of the overall enzymatic process.

Acknowledgements

This work was supported by the U. S. National Science Foundation under grant CHE-9817919.

References and notes

1 D. Gerber, P. Chongsawangvirod, A. K. Leung and L. A. Ochrymowycz, *J. Org. Chem.*, 1977, **42**, 2644.
2 R. S. Glass, G. S. Wilson and W. N. Setzer, *J. Am. Chem. Soc.*, 1980, **102**, 5068.
3 W. N. Setzer, C. A. Ogle, G. S. Wilson and R. S. Glass, *Inorg. Chem.*, 1983, **22**, 266.
4 (*a*) C. Pomp, S. Drueke, H.-J. Küppers, K. Wieghardt, C. Kruger, B. Nuber and J. Weiss, *Z. Naturforsch., Teil B*, 1988, **43**, 299; (*b*) H.-J. Küppers, K. Wieghardt, B. Nuber and J. Weiss, *Z. Anorg. Allg. Chem.*, 1989, **577**, 155; (*c*) H.-J. Küppers and K. Wieghardt, *Polyhedron*, 1989, **8**, 1770; (*d*) H.-J. Küppers, K. Wieghardt, S. Steenken, B. Nuber and J. Weiss, *Z. Anorg. Allg. Chem.*, 1989, **573**, 43; (*e*) H. Elias, G. Schmidt, H.-J. Küppers, M. Saher, K. Wieghardt, B. Nuber and J. Weiss, *Inorg. Chem.*, 1989, **28**, 3021; (*f*) H.-J. Küppers, B. Nuber, J. Weiss and S. R. Cooper, *J. Chem. Soc., Chem. Commun.*, 1990, 979; (*g*) D. J. White, H.-J. Küppers, A. J. Edwards, D. J. Watkin and S. R. Cooper, *Inorg. Chem.*, 1992, **31**, 5321.
5 H. Doine and T. W. Swaddle, *Can. J. Chem.*, 1990, **68**, 2228.
6 H. Doine and T. W. Swaddle, *Inorg. Chem.*, 1991, **30**, 1858.
7 M. Matsumoto, M. Itoh, S. Funahashi and H. D. Takagi, *Can. J. Chem.*, 1999, **77**, 1638.
8 Sanaullah, K. Kano, R. S. Glass and G. S. Wilson, *J. Am. Chem. Soc.*, 1993, **115**, 592.
9 M. J. Martin, J. F. Endicott, L. A. Ochrymowycz and D. B. Rorabacher, *Inorg. Chem.*, 1987, **26**, 3012.
10 M. M. Bernardo, P. V. Robandt, R. R. Schroeder and D. B. Rorabacher, *J. Am. Chem. Soc.*, 1989, **111**, 1224.
11 N. E. Meagher, K. L. Juntunen, C. A. Salhi, L. A. Ochrymowycz and D. B. Rorabacher, *J. Am. Chem. Soc.*, 1992, **114**, 10411.
12 N. Koshino, Y. Kuchiyama, S. Funahashi and H. D. Takagi, *Chem. Phys. Lett.*, 1999, **306**, 291.
13 N. Koshino, Y. Kuchiyama, H. Ozaki, S. Funahashi and H. D. Takagi, *Inorg. Chem.*, 1999, **38**, 3352.
14 N. Koshino, Y. Kuchiyama, S. Funahashi and H. D. Takagi, *Can. J. Chem.*, 1999, **77**, 1498.
15 N. Koshino, S. Itoh, Y. Kuchiyama, S. Funahashi and H. D. Takagi, *Inorg. React. Mech.*, 2000, **2**, 93.

16 Sanaullah, H. Hungerbühler, C. Schöneich, M. Morton, D. G. Vander Velde, G. S. Wilson, K.-D. Asmus and R. S. Glass, *J. Am. Chem. Soc.*, 1997, **119**, 2134.
17 G. H. Leggett, B. C. Dunn, A. M. Q. Vande Linde, L. A. Ochrymowycz and D. B. Rorabacher, *Inorg. Chem.*, 1993, **32**, 5911.
18 N. E. Meagher, K. L. Juntunen, M. J. Heeg, C. A. Salhi, B. C. Dunn, L. A. Ochrymowycz and D. B. Rorabacher, *Inorg. Chem.*, 1994, **33**, 670.
19 C. A. Salhi, Q. Yu, M. J. Heeg, N. M. Villeneuve, K. L. Juntunen, R. R. Schroeder, L. A. Ochrymowycz and D. B. Rorabacher, *Inorg. Chem.*, 1995, **34**, 6053.
20 B. C. Dunn, L. A. Ochrymowycz and D. B. Rorabacher, *Inorg. Chem.*, 1997, **36**, 3253.
21 N. M. Villeneuve, R. R. Schroeder, L. A. Ochrymowycz and D. B. Rorabacher, *Inorg. Chem.*, 1997, **36**, 4475.
22 P. Wijetunge, C. P. Kulatilleke, L. T. Dressel, M. J. Heeg, L. A. Ochrymowycz and D. B. Rorabacher, *Inorg. Chem.*, 2000, **39**, 2897.
23 K. Krylova, C. P. Kulatilleke, M. J. Heeg, C. A. Salhi, L. A. Ochrymowycz and D. B. Rorabacher, *Inorg. Chem.*, 1999, **38**, 4322.
24 (*a*) C. M. Groeneveld, M. C. Ouwerling, C. Erkelens and G. W. Canters, *J. Mol. Biol.*, 1988, **200**, 189; (*b*) C. M. Groeneveld, S. Dahlin, B. Reinhammar and G. W. Canters, *J. Am. Chem. Soc.*, 1987, **109**, 3247; (*c*) G. W. Canters, H. A. O. Hill, N. A. Kitchen and E. T. Adman, *J. Magn. Reson.*, 1984, **57**, 1; (*d*) S. Dahlin, B. Reinhammar and M. T. Wilson, *Biochem. J.*, 1984, **218**, 609; (*e*) A. Lommen and G. W. Canters, *J. Biol. Chem.*, 1990, **265**, 2768; (*f*) P. Kyritsis, C. Dennison, W. J. Ingledew, W. McFarlane and A. G. Sykes, *Inorg. Chem.*, 1995, **34**, 5370.
25 P. J. Blower and S. R. Cooper, *Inorg. Chem.*, 1987, **26**, 2009.
26 L. L. Diaddario, Jr., L. A. Ochrymowycz and D. B. Rorabacher, *Inorg. Chem.*, 1992, **31**, 2347.
27 B. J. Hathaway, D. G. Holah and J. D. Postlethwaite, *J. Chem. Soc.*, 1961, 3215.
28 L. Aronne, B. C. Dunn, J. R. Vyvyan, C. W. Souvignier, M. J. Mayer, T. A. Howard, C. A. Salhi, S. N. Goldie, L. A. Ochrymowycz and D. B. Rorabacher, *Inorg. Chem.*, 1995, **34**, 357.
29 B. C. Dunn, L. A. Ochrymowycz and D. B. Rorabacher, *Inorg. Chem.*, 1995, **34**, 1954.
30 E. L. Yee, R. J. Cave, K. L. Guyer, P. D. Tyma and M. J. Weaver, *J. Am. Chem. Soc.*, 1980, **101**, 1131.
31 H.-M. Koepp, H. Wendt and H. Strehlow, *Z. Elektrochem.*, 1960, **64**, 483.
32 E. A. Ambundo, M.-V. Deydier, A. J. Grall, N. Aguera-Vega, L. T. Dressel, T. H. Cooper, M. J. Heeg, L. A. Ochrymowycz and D. B. Rorabacher, *Inorg. Chem.*, 1999, **38**, 4233; see footnote 66.
33 A recent neutron diffraction study has indicated that hydrated Cu(II) ion may be five-coordinate: A. Pasquarello, I. Petri, P. S. Salmon, O. Parisel, R. Car, E. Toth, D. H. Powell, H. E. Fischer, L. Helm and A. E. Merbach, *Science*, 2001, **291**, 856.
34 R. S. Glass, L. K. Steffen, D. D. Swanson, G. S. Wilson, R. Degelder, R. A. G. DeGraaff and J. Reedijk, *Inorg. Chim. Acta*, 1993, **207**, 241.
35 H. McConnell and N. Davidson, *J. Am. Chem. Soc.*, 1950, **72**, 3164; *cf*. H. A. Benesi and J. H. Hildebrand, *J. Am. Chem. Soc.*, 1949, **71**, 2703.
36 L. S. W. L. Sokol, L. A. Ochrymowycz and D. B. Rorabacher, *Inorg. Chem.*, 1981, **20**, 3189.
37 J. I. Steinfeld, J. S. Francisco and W. L. Hase, *Chemical Kinetics and Dynamics*, Prentice-Hall, Upper Saddle River, NJ, USA, 2nd edn., 1999, pp. 23–24.
38 When the formation of $Cu^{II}L$ was complete, the $Cu^{II}L$ absorbance could be observed to decrease (at 374 nm) and the $Cu^{II}L_2$ absorbance to increase (at 445 nm).
39 It is noteworthy that this value for k_{EC} is nearly identical to the value obtained previously for Cu^{II} reacting with [14]aneS$_4$: k_f = 1.3 × 10^5 M^{-1} s^{-1}: L. L. Diaddario, Jr., L. A. Ochrymowycz and D. B. Rorabacher, *Inorg. Chem.*, 1992, **31**, 2347.
40 K. Krylova, K. D. Jackson, J. A. Vroman, A. J. Grall, M. R. Snow, L. A. Ochrymowycz and D. B. Rorabacher, *Inorg. Chem.*, 1997, **36**, 6216.
41 In aqueous solution it has been estimated that $K_{Cu^{II}L}$ is only 0.04 M^{-1} for dimethyl sulfide as a ligand (as compared to K_{EC} = 1.3 × 10^4 M^{-1} for [9]aneS$_3$): E. A. Ambundo, M.-V. Deydier, L. A. Ochrymowycz and D. B. Rorabacher, *Inorg. Chem.*, 2000, **39**, 1171.
42 By contrast, the electrospray mass spectra for solutions containing Cu(I) and the related [9]aneS$_2$O ligand showed nearly equivalent amounts of $CuL{\cdot}CH_3CN^+$ and CuL_2^+ in solutions containing equivalent amounts of Cu(I) and ligand. This is presumably due to the fact that the Cu(I)–O bond is very weak and each of the ligand molecules is coordinated to the Cu(I) *via* the two sulfur donor atoms: G. J. Grant, D. F. Glass, M. W. Jones, K. D. Loveday, W. T. Pennington, G. L. Schimek, C. T. Eagle and D. G. VanDerveer, *Inorg. Chem.*, 1998, **37**, 5299.
43 J. H. Christie, J. A. Turner and R. A. Osteryoung, *Anal. Chem.*, 1977, **49**, 1899.
44 M. M. Bernardo, R. R. Schroeder and D. B. Rorabacher, *Inorg. Chem.*, 1991, **30**, 1241.
45 Q. Yu, C. A. Salhi, E. A. Ambundo, M. J. Heeg, L. A. Ochrymowycz and D. B. Rorabacher, *J. Am. Chem. Soc.*, 2001, **123**, 5720.
46 R. A. Marcus and N. Sutin, *Biochim. Biophys. Acta*, 1985, **811**, 265.
47 G. M. Brown and N. Sutin, *J. Am. Chem. Soc.*, 1979, **101**, 883.
48 D. M. Stanbury, O. Haas and H. Taube, *Inorg. Chem.*, 1980, **19**, 518.
49 E. I. Seddon and K. R. Seddon, *Chemistry of Ruthenium*, Elsevier, New York, 1984, p. 444.
50 G. M. Bryant, J. E. Fergusson and H. K. H. Powell, *Aust. J. Chem.*, 1971, **24**, 257.
51 I. Ruff and M. Zimonyi, *Electrochim. Acta*, 1973, **18**, 515.
52 W. W. Brandt and G. F. Smith, *Anal. Chem.*, 1949, **21**, 1313.
53 M. J. Sisley and R. B. Jordan, *Inorg. Chem.*, 1992, **31**, 2880.
54 E. A. Ambundo, L. A. Ochrymowycz and D. B. Rorabacher, *Inorg. Chem.*, 2001, **40**, 5133.